

# Oscillation Mechanics of the Respiratory System: Applications to Lung Disease

David W. Kaczka<sup>a,b,\*</sup> & Raffaele L. Dellacá<sup>c</sup>

<sup>a</sup>Department of Anesthesia, Harvard Medical School, Boston, Massachusetts, USA; <sup>b</sup>Department of Anesthesia, Critical Care, and Pain Medicine, Beth Israel Deaconess Medical Center, Boston, Massachusetts, USA;

<sup>c</sup>Dipartimento di Bioingegneria, Politecnico di Milano University, Milano, Italy

\*Address correspondence to: David W. Kaczka, Department of Anesthesiology, Critical Care, and Pain Medicine, Beth Israel Deaconess Medical Center, 330 Brookline Avenue, Dana 717A, Boston, MA 02215; Tel.: 617-667-0142; Fax: 617-667-1500; dkaczka@bidmc.harvard.edu

**ABSTRACT:** Since its introduction in the 1950s, the forced oscillation technique (FOT) and the measurement of respiratory impedance have evolved into powerful tools for the assessment of various mechanical phenomena in the mammalian lung during health and disease. In this review, we highlight the most recent developments in instrumentation, signal processing, and modeling relevant to FOT measurements. We demonstrate how FOT provides unparalleled information on the mechanical status of the respiratory system compared to more widely used pulmonary function tests. The concept of mechanical impedance is reviewed, as well as the various measurement techniques used to acquire such data. Emphasis is placed on the analysis of lower, physiologic frequency ranges (typically less than 10 Hz) that are most sensitive to normal physical processes as well as pathologic structural alterations. Various inverse modeling approaches used to interpret alterations in impedance are also discussed, specifically in the context of three common respiratory diseases: asthma, chronic obstructive pulmonary disease, and acute lung injury. Finally, we speculate on the potential role for FOT in the clinical arena.

**KEY WORDS:** forced oscillations, respiratory mechanics, asthma, chronic obstructive pulmonary disease, acute lung injury

## I. INTRODUCTION

The primary function of the respiratory system is gas exchange, which relies on the movement of air to and from the alveoli, a physiologic process known as ventilation. Ventilation requires driving pressures to overcome the resistive, elastic, and (under special circumstances) inertial components of the lungs and chest wall. The magnitudes of these components are often used as indices of energy dissipation and storage associated with the process of ventilation and the work of breathing. The resistance and elastance of the respiratory system exhibit dependence on breathing frequency across all mammalian species due to several mechanical processes, such as tissue viscoelasticity,<sup>1</sup> parallel and serial time-constant heterogeneity,<sup>2,3</sup> and collateral ventilation.<sup>4,5</sup> Since its introduction in the 1950s, the forced oscillation technique (FOT) has evolved into a useful method for determining these processes' relative roles in ventilation during health

and disease, as well as their unique and distinct contributions to the mechanical behavior of the lung. With FOT, time-varying flows of one or more frequencies are forced into the lungs at the airway opening. The complex ratio of the resulting pressure to the delivered flow is defined as the mechanical input impedance,  $Z$ . Experimental studies in both humans and animals, as well as simulation studies with morphometric models, indicate that the frequency-dependent features of  $Z$  permit inferences on the distribution of obstruction in the airways<sup>6,7</sup> and in some situations, allow the partitioning of airway and parenchymal mechanical properties.<sup>8–10</sup> Such information may provide the clinician with much needed insight into the pathophysiological mechanisms contributing to compromised lung function and the effectiveness of medical and/or surgical interventions.

Many diseases of the respiratory system manifest themselves as mechanical derangements, which

are usually assessed using various standard tests of pulmonary function.<sup>11</sup> Nonetheless, data from such tests (i.e., plethysmography and maximal effort spirometry) are very nonspecific for identifying pathologic structural alterations in the lungs. In contrast, impedance data, especially when interpreted with models unique to specific physiologic mechanisms and/or pathologic alterations, do provide very unique insight into structure–function relationships.<sup>12–15</sup> Moreover, FOT approaches require minimal subject cooperation, a considerable advantage when dealing with pediatric or critically ill patients. Despite the diagnostic potential of FOT, there has been relatively little effort to incorporate its use into routine clinical practice.<sup>16</sup> This may reflect the technical difficulties associated with its measurements, as well as obscure physiological interpretations in the presence of highly nonlinear and pathologic processes such as dynamic airway compression,<sup>17–19</sup> intratidal derecruitment,<sup>20</sup> and parenchymal overdistention.<sup>21</sup> Moreover, clinically practical and efficient methods to measure impedance in patients have remained elusive until recently.<sup>18,22–25</sup>

This review emphasizes the authors' experience with FOT, as well as the most recent developments in relevant instrumentation, signal processing, and modeling. Similar to earlier reviews on the topic,<sup>26–30</sup> this article illustrates how FOT provides unparalleled information on the mechanical status of the respiratory system compared to more widely used measures of pulmonary function. The concept of mechanical impedance and the various measurement techniques used to acquire such data are reviewed. Emphasis is placed on the analysis of lower, physiologic frequency ranges (typically less than 10 Hz) that are particularly sensitive to normal physical processes as well as pathologic structural alterations. Various inverse modeling approaches used to interpret alterations in impedance are also discussed, specifically in the context of three common respiratory diseases: asthma, chronic obstructive pulmonary disease (COPD), and acute lung injury (ALI). Finally, future developments for FOT and its use in the clinical arena are considered.

## II. CONCEPT OF MECHANICAL IMPEDANCE

FOT was first introduced in the 1950s by Dubois et al. to measure the mechanical impedance of the respiratory system.<sup>31</sup> The concept of mechanical impedance, similar to electrical impedance in AC circuit analysis, is grounded in the theory of linear systems,<sup>32,33</sup> in which a black-box representation of the respiratory system embodies a precise quantitative relationship between specific pressures and flows measured during oscillatory motion. Presumably, this relationship arises from the resistive, inertial, and elastic contributions of the lungs and/or chest wall. Impedance ( $Z$ ) is defined as the complex ratio of pressure ( $P$ ) to flow ( $\dot{V}$ ) as a function of oscillation frequency ( $\omega$ ):

$$Z(\omega) = \frac{P(\omega)}{\dot{V}(\omega)} \quad (1)$$

In polar notation,  $Z$  is expressed with a magnitude, to account for relative differences in the amplitudes between the sinusoidal pressures and flows, as well as a phase angle, to account for time shifts (i.e., leads or lags) between them.<sup>34</sup> More commonly,  $Z$  is expressed in Cartesian coordinates in the complex plane, with resistive ( $R$ ) and reactive ( $X$ ) components, allowing for separation of those processes associated with energy dissipation and energy storage, respectively:

$$Z(\omega) = R(\omega) + jX(\omega) \quad (2)$$

where  $j$  is the unit imaginary number, defined as  $\sqrt{-1}$ . For the respiratory system, resistance arises from the viscous flow of gas through the airways,<sup>35</sup> as well as energy losses associated with the deformation of the parenchyma<sup>36</sup> and chest wall.<sup>37</sup> For frequencies below 10 Hz, reactance is comprised of an inertial component ( $I$ ) due to acceleration of gas in the central airways, as well as an elastic component ( $E$ ) due to the recoil of the parenchyma and chest wall:

$$X(\omega) = \omega I - \frac{E}{\omega} \quad (3)$$

Equation 3 demonstrates that a specific frequency exists, termed the resonant frequency ( $\omega_o$ ), for which the reactance is zero and impedance is due solely to resistive losses. Rearranging Eq. 3 and solving for  $X(\omega) = 0$ , we obtain

$$\omega_o = \sqrt{\frac{E}{I}} \quad (4)$$

At  $\omega_o$ , the magnitude of impedance is at a minimum. Over low frequencies (i.e.,  $\omega \ll \omega_o$ ), inertia has a negligible contribution to impedance, and the reactance is determined largely by the recoil of the parenchymal or respiratory tissues. In this situation, it is common practice to express reactance as elastance as a function of frequency.<sup>38–40</sup>

$$E(\omega) = -\omega X(\omega) \quad (5)$$

Generally, mechanical impedance is measured in one of two ways. First, pressure oscillations may be generated around the body surface ( $P_{bs}$ ) while measuring the resulting flow at the airway opening ( $\dot{V}_{ao}$ ). Here the subjects' torso, or entire body, is encased in an airtight chamber (Figure 1B). The ratio between  $P_{bs}$  and  $\dot{V}_{ao}$  is termed *transfer impedance* ( $Z_{tr}$ ).<sup>31</sup> Alternatively, oscillatory flows may be presented to the airway opening while simultaneously measuring the resulting airway opening pressure ( $P_{ao}$ ) relative to atmosphere. The ratio between  $P_{ao}$  and  $\dot{V}_{ao}$ , when the chest wall is intact, is the *input impedance* of the *total respiratory system* ( $Z_{rs}$ ). If  $P_{ao}$  is measured relative to the pressure at the pleural surface ( $P_{pl}$ , often approximated using an esophageal balloon in the living subject), then the ratio  $(P_{ao} - P_{pl})/\dot{V}$  is the input impedance of the lungs alone ( $Z_L$ ). Given that  $P_{ao}$  and  $\dot{V}_{ao}$  are usually the most easily accessible and transduced variables in the clinical setting, this review concentrates on the more intuitive input impedance alone.

Mechanical impedance reflects very different physical processes depending on the frequency range studied or the presence of lung disease. Traditionally, input impedance data was acquired in the range of 4–32 Hz, as this allowed the human subject to breath spontaneously through a high-inertance tube to-and-from ambient during the measurement, with minimal band-overlap between the spectral

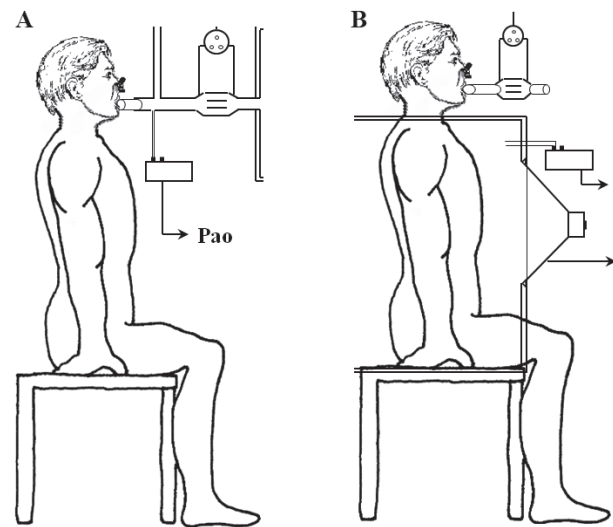


**FIGURE 1:** Two methods for measuring impedance with forced oscillations. (A) Input impedance ( $Z_{in}$ ) technique, in which oscillatory ( $\dot{V}_{ao}$ ) is applied at the mouth or trachea while measuring airway opening pressure ( $P_{ao}$ ). (B) Transfer impedance ( $Z_{tr}$ ) technique, in which pressure oscillations are applied at the body surface ( $P_{bs}$ ) while flow at the airway opening ( $\dot{V}_{ao}$ ) is measured.

energy of the natural breathing waveforms and the imposed oscillations.<sup>27,29</sup> After high-pass filtering of the measured flow and pressures signals, impedance can be computed using various Fourier Transform methods.<sup>34,41,42</sup> While simple to acquire, impedance data acquired within this bandwidth is the least informative in terms of physiology.<sup>43</sup> Over this frequency range, the real part of impedance is generally constant with frequency, while the imaginary part increases monotonically with frequency, behaviors consistent with simple, constant resistive–inertial–compliant properties of the respiratory system.<sup>29,31</sup>

By contrast, input impedance measured over the 0.1–10 Hz bandwidth reflects far more interesting phenomena. For example, parallel time constant heterogeneity,<sup>2</sup> airway wall distensibility,<sup>3</sup> parenchymal viscoelasticity,<sup>44–46</sup> expiratory flow limitation,<sup>47</sup> and collateral ventilation<sup>4</sup> have the greatest influence on input impedance over this lower frequency range. A typical impedance spectrum from 0.156 to 8.1 Hz, expressed as lung resistance ( $R_L$ ) and elastance ( $E_L$ ), is shown for a healthy awake human subject in Figure 2. Both  $R_L$  and  $E_L$  are strongly dependent on

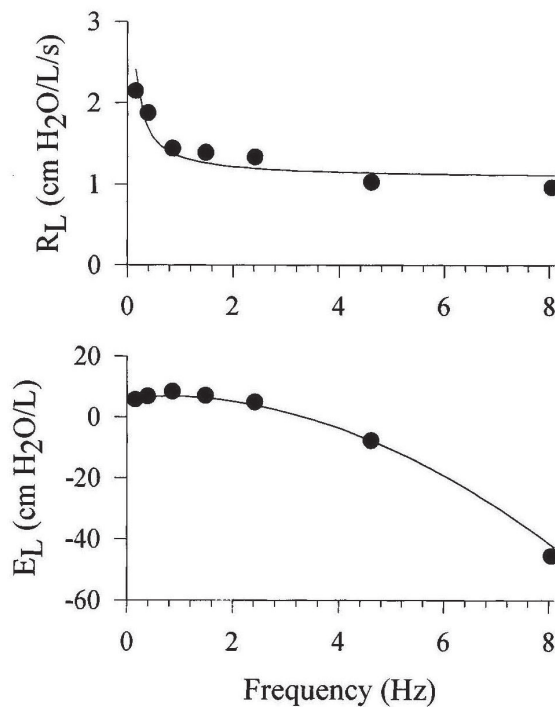


**FIGURE 2:** Lung resistance ( $R_L$ ) and elastance ( $E_L$ ) versus frequency in a representative healthy human subject under baseline conditions. Shown are the actual measured data (symbols) along with corresponding model fit (lines) using Eq. 9. Modified from Kaczka et al.,<sup>38</sup> with permission.

oscillation frequency, primarily due to viscoelasticity of the parenchymal tissues.<sup>48</sup> Specifically,  $R_L$  shows a frequency-dependent drop from 0.156 to 1.0 Hz and attains a plateau by 2–4 Hz. The  $E_L$  increases slightly with frequency between 0.156 and 1.0 Hz, then decreases at higher frequencies and becomes negative due to the inertia of gas in the central airways. Figure 3 shows  $R_L$  and  $E_L$  spectra for a healthy subject at baseline and following small and large doses of inhaled methacholine, a cholinergic agonist that causes bronchoconstriction. With mild bronchoconstriction,  $R_L$  slightly increases compared to baseline at all frequencies, while  $E_L$  changes minimally. For the more moderate level of bronchoconstriction,  $R_L$  becomes highly elevated at all frequencies relative to the baseline. While  $E_L$  increases slightly for frequencies below 1 Hz, it demonstrates a strong positive frequency-dependence above 1 Hz. The physiologic mechanisms contributing to such observed behavior

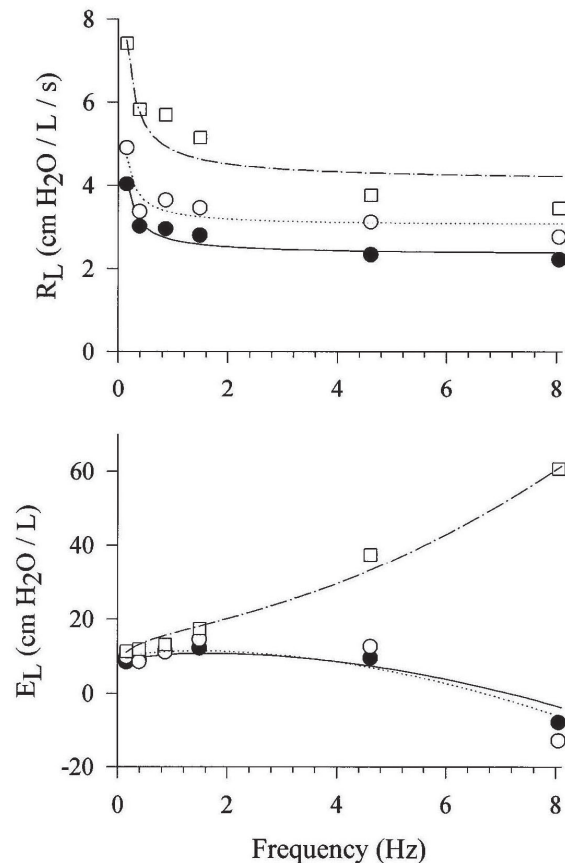


**FIGURE 3:** Lung resistance ( $R_L$ ) and elastance ( $E_L$ ) versus frequency in a representative human subject at baseline (filled circles) and following inhalation of methacholine aerosol at concentrations of 0.025 mg/ml (open circles) and 20.0 mg/ml (open squares). Also shown are corresponding model fits using Eq. 9 (lines). Modified from Kaczka et al.,<sup>38</sup> with permission.

in  $R_L$  and  $E_L$  are discussed below in the context of inverse modeling.

### III. MEASUREMENT TECHNIQUES

#### A. Instrumentation

A key requirement for any study of oscillatory mechanics of the respiratory system is a device capable of generating high-fidelity pressure or flow excitations to which the lungs and/or chest wall will be exposed. For frequencies within the com-



monly used 4–32 Hz bandwidth, this can usually be accomplished with a loudspeaker system with appropriate dynamic response,<sup>34,49</sup> which may be placed in parallel with a mechanical ventilator or other respiratory assist devices.<sup>50–53</sup> Lower excitation frequencies, especially those surrounding physiologic breathing rates, require relatively load-independent generators with sufficient dynamic responses that encompass such bandwidths. Measurements at these lower frequencies have traditionally been obtained with reciprocating piston-pumps actuated by servo-controlled linear motors.<sup>31,54,55</sup> More recently, low-frequency pressure waveforms have been generated with considerable fidelity using a proportional solenoid valve incorporated into a closed-loop system, as this allows for fine control of both mean and oscillatory components of airway pressure.<sup>12,40,56</sup> However in awake subjects, such low-frequency measurements require considerable training and cooperation to allow complete relaxation of the diaphragm and chest wall muscles,<sup>38,39,57</sup> which may be impractical for patients with lung disease.<sup>22</sup> Many of these forced oscillation systems can easily be incorporated into existing ventilator platforms in the operating room or intensive care unit, allowing for bedside assessment of respiratory mechanics with minimal disruption of ventilatory support.<sup>51,52</sup>

Recent advances in digital microelectronics have lead to the availability of powerful microprocessors at very low cost, allowing for simple, robust, and portable designs for FOT devices. Rigau et al. showed that FOT was potentially applicable to home monitoring.<sup>58,59</sup> A recent study by Dellaca et al. demonstrated the feasibility of using an inexpensive FOT system for real-time data acquisition, processing, and Internet streaming.<sup>24</sup> These preliminary studies support the idea that FOT could potentially be used for daily home assessment of obstructive lung diseases and the management of their exacerbations.

Another necessary requirement for FOT is the accurate measurement of oscillatory signals during the excitation, which must be electrically transduced to allow for necessary filtering, display, digitization, and storage of data. This requires knowledge of a particular transducer's linearity, measurement range, and frequency response.<sup>60,61</sup> Fundamental to any study

of oscillatory mechanics of the respiratory system is the measurement of pressure, which may be obtained at the airway opening,<sup>38</sup> around the body surface,<sup>31</sup> within the esophagus,<sup>62</sup> or even within the airways or alveoli.<sup>63–65</sup> Any of these pressures may be transduced relative to atmosphere by differential sensors with one of the two inputs left open to ambient air. Traditionally, variable reluctance transducers have been used for FOT measurements, as they have both high sensitivity and adequate frequency response.<sup>66,67</sup> These transducers behave similarly to an AC transformer, in which a pressure-sensing diaphragm made of magnetically permeable material is mounted between two induction coils. The primary coil is excited by an AC current of several kHz, which induces a voltage in the secondary coil. When the diaphragm moves in response to a differential pressure, the deformation affects the efficiency of induction in the secondary coil. This results in an alteration in the magnetic flux linkage between the coils, which can be detected by appropriate electronic circuits. More recently, improvements in semiconductor production have led to the development of reliable, accurate, and inexpensive piezoresistive transducers, in which the electrical resistance of the sensing diaphragm changes in response to an applied force. These small devices also have reduced internal gas volume and diaphragm compliance, resulting in an even better frequency response compared to variable reluctance transducers.

Oscillatory flow measurements are commonly made with pneumotachographs, which may be of the mesh screen or capillary tube type (e.g., Fleisch) variety.<sup>68</sup> These devices produce a pressure drop that is ideally linearly related to flow according to Poiseuille's Law.<sup>69</sup> The effective mechanical resistance offered by the pneumotachograph, and hence its corresponding pressure drop, is dependent not only on the geometry of its connecting conduits but also on the viscosity of the particular species of gas being measured.<sup>70</sup> Several calibrations may therefore be required if flow measurements are to be made under varying oxygen levels or different concentrations of inhaled anesthetics.<sup>71</sup> Moreover, all pneumotachographs have unique dynamic responses that systematically distort the measured magnitude and phase of any

oscillatory flow, depending on frequency.<sup>72</sup> This may require additional dynamic compensation, especially for frequencies above 20 Hz.<sup>73–75</sup> In addition, because the measured flow is based on a differential pressure drop, pneumotachographs may require correction for transducer asymmetry and finite common-mode rejection ratio.<sup>76</sup> Finally for prolonged measurements, the pneumotachograph should contain a heating element to minimize the error associated with condensation,<sup>70</sup> although this will not prevent it from becoming clogged with respiratory secretions. Alternatively, hot-wire anemometers can also measure oscillatory flows over a much broader bandwidth.<sup>77,78</sup> In contrast to pneumotachography, which relies on the measurement of a pressure drop across a fluid resistive element, hot-wire anemometry relies on changes in the electrical resistance of a current-carrying filament.<sup>79</sup> As gas flows past the wire, its temperature decreases, resulting in a corresponding change in its electrical conductivity which can be measured with a standard Wheatstone bridge circuit.<sup>80</sup>

## B. Signal Processing

To calculate impedance spectra from oscillatory flow and pressure waveforms, several signal processing techniques can be used. The simplest and most direct is to excite the respiratory system at one discrete frequency while the subject remains apneic, and then determine the value of impedance from the corresponding pressure and flow (using Eq. 1) at this frequency. By continually forcing the respiratory system with different discrete frequencies, values of the impedance can be obtained over a particular frequency range.<sup>81–83</sup> Obviously this method becomes quite time consuming, depending on the desired frequency resolution and range, and is impractical for serial impedance measurements to assess the temporal dynamics of a pharmacologic agonist.<sup>84</sup> A more efficient method involves exciting the system with broadband waveforms that simultaneously contain all frequencies of interest. This can be done using multiple sinusoids<sup>85</sup> or small-amplitude random noise.<sup>34</sup> The input flow and output pressure signals can then be spectrally decomposed into their indi-

vidual frequency components using standard Fourier analysis,<sup>41,86,87</sup> from which the value of the impedance can be determined at each particular frequency. When multi-frequency forcing signals are used, the spectra are most reliably estimated as

$$Z(\omega) = \frac{G_{P\dot{V}}(\omega)}{G_{\dot{V}\dot{V}}(\omega)} \quad (6)$$

where  $G_{P\dot{V}}$  is the cross-power spectrum between pressure and flow and  $G_{\dot{V}\dot{V}}$  is the auto-power spectrum of flow. The estimates of  $G_{P\dot{V}}$  and  $G_{\dot{V}\dot{V}}$  are obtained by averaging the periodograms computed from several data segments, with each segment containing one or more forcing periods.<sup>41</sup> The advantage of this periodogram approach is that it readily yields the so-called coherence function ( $\gamma^2$ ) between flow and pressure at each frequency:

$$\gamma^2(\omega) = \frac{|G_{P\dot{V}}^2(\omega)|}{G_{\dot{V}\dot{V}}(\omega)G_{PP}(\omega)} \quad (7)$$

The coherence can be used as an index of causality between the input flow and output pressure of the respiratory system<sup>88</sup> and ranges in value between 0 and 1. For the purposes of assessing the quality of impedance data, values less than 0.95 are usually discarded.<sup>38,39</sup> Nonlinearities in the respiratory system may result in a distorted estimate of  $Z$  or  $\gamma$ ,<sup>2,88,89</sup> although such distortions can be minimized by excitation with frequencies that are noninteger multiples of the fundamental frequency<sup>90</sup> or that are mutually prime.<sup>38,91,92</sup>

For low frequencies surrounding typical breathing rates, small-amplitude forcings, which require the awake subject to remain apneic,<sup>57</sup> may be impractical for patients with significant lung disease. Moreover their use in intubated patients usually requires discontinuation of artificial ventilatory support,<sup>51</sup> although attempts have been made to extract impedance data at multiple frequencies using standard volume-cycled waveforms.<sup>87,93–95</sup> These attempts have been largely unsuccessful due to the limited spectral energy in such waveforms above the fundamental frequency, yielding poor signal-to-noise ratio at the higher harmonics. To overcome these limitations, Lutchen et al. proposed the use of an optimal ventilator waveform (OVW)

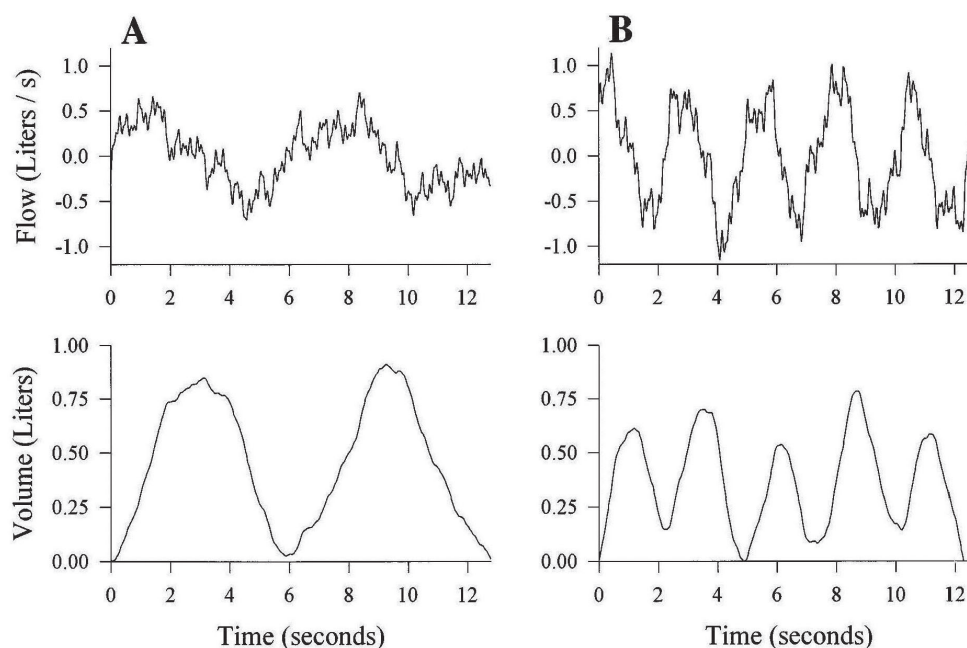


**FIGURE 4:** Flow and volume tracings for two types of optimal ventilator waveforms (OVWs) with 12.8-second periods. (A) OVW in which peak spectra energy occurs at 0.15625 Hz, with two distinct physiologic breaths per period. (B) OVW in which peak spectra energy occurs at 0.390625 Hz, with five distinct physiologic breaths per period and lower frequency modulation at 0.15625 Hz. Modified from Kaczka et al.,<sup>38</sup> with permission.

as a more practical and efficient method for measuring low frequency input impedance in humans.<sup>92</sup> The OVW is a broadband oscillatory flow input designed to estimate the frequency response of the lungs during tidal-like excursions (Figure 4A). The signal-to-noise ratio of this waveform is enhanced for frequencies above the fundamental frequency, and its spectral energy is concentrated only at specific frequencies to minimize harmonic distortions in the resulting pressure.<sup>91</sup> In a subsequent study, Kaczka et al. designed a variation of this original OVW to make it more amenable for awake human subjects.<sup>38</sup> Here the magnitude spectrum of the waveform is adjusted such that the primary frequency of ventilation was more comfortable for the subject but was modulated by smaller-amplitude energy at lower frequencies (Figure 4B). While the OVW is useful for patients with mild-to-moderate obstructions who can be trained to relax their chest wall muscles,<sup>38,39</sup> it is not appropriate for use in severely obstructed patients.<sup>22</sup> Moreover, because the OVW is delivered

via a closed system, a bias flow of fresh gas must be delivered into the breathing circuit to ensure sufficient gas exchange.<sup>38</sup>

One drawback of using the above Fourier analysis method to estimate respiratory impedance is the assumption that the system is stationary during the measurement period. However, when a discrete sinusoidal forcing is used with a frequency sufficiently faster than breathing rates (i.e., 5–10 Hz), it is possible to compute impedance with a high temporal resolution and track within-breath variations of respiratory mechanical properties. In this case the impedance can be obtained from algorithms based on cross correlation,<sup>96,97</sup> fast Fourier transforms,<sup>53,98</sup> or various recursive and nonrecursive least-squares techniques.<sup>47,87,99–102</sup> Within-breath analysis of impedance is potentially valuable for a wide range of clinical applications, such as detection of obstructive sleep apnea and expiratory flow limitation,<sup>25,47,103</sup> the evaluation of lung mechanics during positive pressure

ventilation,<sup>104</sup> and the examination of the effects of deep inspirations on airway constriction.<sup>101,105,106</sup>

#### IV. INVERSE MODELING OF IMPEDANCE

One way to characterize the relationship between pressure and flow of the respiratory system is to develop an electromechanical analogue that is structurally sensible and can simulate actual impedance data. Ideally, the parameters of such a model should be related to the basic physiologic properties of the respiratory system. Input impedance within the commonly used 4–32 Hz bandwidth can be reasonably predicted ( $\hat{Z}$ ) with simple linear resistance ( $R$ ), inertance ( $I$ ), and elastance ( $E$ ) elements in series, all of which are assumed to be constant with frequency<sup>31</sup>:

$$\hat{Z}(\omega) = R + j\omega I + \frac{E}{j\omega} \quad (8)$$

Nonetheless, such a model is far too simple to characterize dynamic mechanical behavior for most pathologies of the respiratory system, especially for frequencies below 4 Hz where natural breathing occurs. As already noted, dependence of  $R$  and  $E$  on breathing frequency has been observed across all mammalian species in both health and disease, and many different but physically plausible mechanisms can account for such dependencies. Thus, more complicated models must be used to mimic many of these phenomena.<sup>33</sup>

When pressures across the airways and within the parenchyma are sampled using alveolar capsules in healthy mammalian lungs,<sup>64</sup> parenchymal tissue resistance decreases nearly hyperbolically with increasing frequency, while airway resistance remains fairly constant.<sup>107–109</sup> Such behavior is consistent with the parenchyma being a viscoelastic material.<sup>48</sup> Given these distinct frequency responses of the airways and tissues, Hantos et al.<sup>110</sup> described  $Z_L$  with a frequency-domain variant of Hildebrandt's stress-relaxation model,<sup>111</sup> consisting of a homogeneous airways compartment containing an airway resistance ( $R_{aw}$ ) and inertance ( $I_{aw}$ ) elements leading to a viscoelastic, constant-phase tissue compartment (Figure

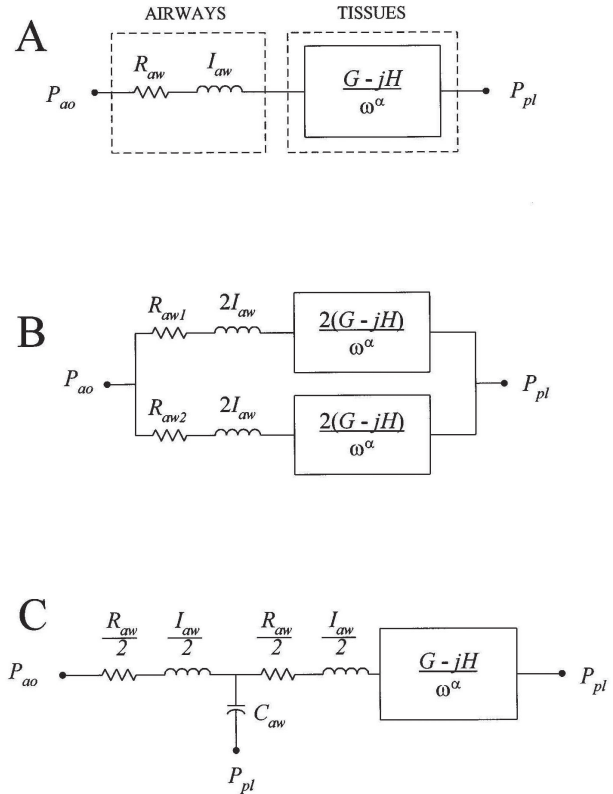


**FIGURE 5:** Various models used to describe oscillatory mechanics of the lungs. (A) Model consisting of homogeneous airways with resistive ( $R_{aw}$ ) and inertial ( $I_{aw}$ ) components, in series with 'constant-phase' viscoelastic tissues containing parameters for tissue damping ( $G$ ) and tissue elastance ( $H$ ). (B) Inhomogeneous airways model with two separate parallel pathways, each containing distinct airway resistive parameters ( $R_{aw1}$  and  $R_{aw2}$ ) but identical  $I_{aw}$  parameters and identical tissue compartments. (C) Model containing an airway compliance parameter ( $C_{aw}$ ) to account for the shunting of oscillatory flow into non-rigid airway walls.  $j$ , unit imaginary number;  $\omega$ , angular frequency;  $P_{pl}$ , pleural pressure. Modified from Kaczka et al.,<sup>38</sup> with permission.

5A). This tissue compartment has two parameters: tissue damping ( $G$ ) and tissue elastance ( $H$ ). For this model, the predicted lung impedance ( $\hat{Z}_L$ ) as a function of angular frequency ( $\omega$ ) is given by

$$\hat{Z}_L(\omega) = R_{aw} + j\omega I_{aw} + \frac{G - jH}{\omega^\alpha} \quad (9)$$

where



$$\alpha = \frac{2}{\pi} \tan^{-1} \left( \frac{H}{G} \right) \quad (10)$$

This model has four independent parameters ( $R_{aw}$ ,  $I_{aw}$ ,  $G$ , and  $H$ ) that may be estimated using various nonlinear gradient search algorithms<sup>107,112,113</sup> or recursive multiple linear regression.<sup>33</sup> Moreover, it is compatible with ‘structural-damping,’ which assumes that the ratio of dissipative and elastic processes in the lung parenchyma, referred to as hysteresivity,<sup>36</sup> is constant with frequency and is given by  $\eta = G/H$ . Also consistent with alveolar capsule data,<sup>10,109</sup> the model predicts that parenchymal tissue resistance ( $R_{ti}$ ) decreases quasi-hyperbolically with frequency:

$$R_{ti}(\omega) = \frac{G}{\omega^\alpha} \quad (11)$$

A limitation of this model, however, is the assumption that impedance can be sufficiently described by serial compartments representing homogenous airways and tissues. Such an assumption is not always valid, especially under pathologic conditions for which heterogeneity results in additional frequency-dependence in impedance that is not due to viscoelasticity alone.<sup>9,40,114,115</sup> For example, the subject of Figure 3 experienced widespread peripheral airway constriction following a large dose of inhaled methacholine, which resulted in the shunting of oscillatory flows into the central airway walls.<sup>116,117</sup> Above 1 Hz, the measured  $E_L$  for this subject increases with frequency, as its value approaches the elasticity of the central airway walls.<sup>3</sup> In this case, the model of Eq. 9 can be modified by dividing the homogeneous airway compartment into two equal halves by an additional shunt airway compliance parameter to account for non-rigid airway walls (Figure 5C). Such a model may be more appropriate to describe lung mechanics in patients with severe asthma<sup>39</sup> or COPD,<sup>22</sup> because it mimics this ‘airway shunting’ behavior and more accurately partitions the mechanical behavior of the airways and lung tissues.<sup>38</sup>

To compensate for parallel time-constant inhomogeneities, the homogeneous airways model can also be modified to contain two separate  $R_{aw}$  pathways, both leading to identical constant-phase tissues (Figure 5B). The resulting inhomogeneous

airways model is structurally analogous to a similar two-compartment model first described by Otis et al.,<sup>2</sup> which compartmentalizes the lungs into ‘healthy’ and ‘diseased’ portions. However, a more accurate description of lung mechanical behavior for many different pathologies may be obtained by distributing parallel heterogeneity across an arbitrary number of parallel pathways.<sup>12,40,118–120</sup> Such models allow for stochastic variability in  $R_{aw}$  or  $H$ , depending on whether one seeks to ascribe the variation to airway or tissue heterogeneity, respectively. For example to characterize heterogeneous airway obstruction, we may assume that the distribution of parallel airway resistances can be approximated with a predefined probability density function,  $P(R_{aw})$ , with lower and upper bounds  $R_{aw,min}$  and  $R_{aw,max}$ , respectively. The impedance predicted by such a model is given by

$$\hat{Z}_L(\omega) = \left[ \int_{R_{aw,min}}^{R_{aw,max}} \frac{P(R_{aw})}{R_{aw} + j\omega I_{aw} + \frac{G - jH}{\omega^\alpha}} dR_{aw} \right]^{-1} \quad (12)$$

In contrast to the model described by Eq. 9 with four independent parameters, this model requires the estimation of five parameters ( $R_{aw,min}$ ,  $R_{aw,max}$ ,  $I_{aw}$ ,  $G$ , and  $H$ ). For pathologies associated with heterogeneity in parenchymal mechanics, such as emphysema or acute lung injury, we may assume a similar topology that allows for variations in tissue elastance between  $H_{min}$  and  $H_{max}$ :

$$\hat{Z}_L(\omega) = \left[ \int_{H_{min}}^{H_{max}} \frac{P(H)}{R_{aw} + j\omega I_{aw} + \frac{G - jH}{\omega^\alpha}} dH \right]^{-1} \quad (13)$$

Both of the models described by Eqs. 12 and 13 yield an ‘effective’ airway resistance or tissue elastance from the mean of the distribution function  $P$ . An estimate of the ‘heterogeneity’ of the airways or tissues can be obtained from the standard deviation of  $P$ .<sup>40,118</sup>

While the models described by Eqs. 9, 12, and 13 do not provide any specific information on anatomy or structure, they do have the ability to characterize global dynamic lung function with a minimal number

of physical parameters.<sup>114,118</sup> Of course, the validation of any candidate model of lung mechanics requires reliable information on the structural alterations associated with a particular disease for comparison with model predictions.<sup>12,33,114</sup> Recent studies combining various functional imaging modalities with impedance measurements have yielded tremendous insight into how specific alterations in structure impact mechanical function.<sup>12,13,121–123</sup>

There are limitations with inverse modeling; one cannot expect to extract all of the mechanisms contributing to the frequency-dependent features in  $Z$ , especially when the number of data points fitted is slightly larger than the number of model parameters.<sup>114</sup> While increasing the complexity of the model to account for additional mechanisms may significantly improve the fit to the data, the resulting parameters may become statistically unreliable.<sup>124,125</sup> Moreover, obtaining a model with the best statistical fit to the data does not imply that all of the physiological mechanisms contributing to the frequency dependence of  $Z$  have been accounted. Indeed depending on pathology, many different mechanisms may simultaneously contribute to the respiratory system's mechanical behavior over similar frequency ranges. Nonetheless, inverse modeling is useful in distinguishing which mechanisms *dominate* the impedance data for a specific physiologic state or disease.<sup>12</sup>

## V. ASTHMA

Asthma is a disease characterized by a hyper-responsiveness to a variety of stimuli (e.g., allergens, cold air, exercise, aspirin), resulting in variable airflow obstruction and increased airway resistance. In allergic asthma (the most common form), the airways exhibit hypertrophy of surrounding smooth muscle and mucous glands, along with extensive infiltration by eosinophils. Here, inhaled allergens bind to IgE antibodies on the surface of mast cells within the bronchial mucosa. This antigen–antibody reaction causes mast cells to degranulate and release a variety of inflammatory mediators, such as histamine, neutrophil and eosinophil chemotactic factors,

bradykinin, and others. These mediators result in smooth-muscle contraction and mucus production, as well as increased vascular permeability and edema. The release of mediators from eosinophils (leukotriene  $B_4$  and PAF) result in damage to the bronchial epithelium, causing further bronchoconstriction and mucus secretion via reflex vagal discharge. If these inflammatory processes are left untreated, airway wall remodeling and adventitial thickening can develop, which may attenuate the dynamic tethering forces to which airway smooth muscle is normally subjected during tidal breathing. This decreases the load against which the muscle must shorten, thus further predisposing it to constriction.<sup>126</sup> During asthmatic exacerbations, airway resistance can become highly elevated due to contraction and hypertrophy of airway smooth muscle, mucus plugging, and edema. This elevation in airway resistance can often, though not always, be reversed by inhalation of a  $\beta$ -agonist such as albuterol, which relaxes airway smooth muscle.<sup>127,128</sup>

While asthma has traditionally been considered an airway disease, plethysmographic measurements in asthmatics raised the possibility that parenchymal tissue resistance,  $R_{ti}$ , may also have a significant role in its pathophysiology.<sup>129–131</sup> For example, alveolar capsule studies in different species have reported greater increases in  $R_{ti}$  during histamine or methacholine induced-bronchoconstriction compared to that of  $R_{aw}$ .<sup>132–135</sup> Such alterations in  $R_{ti}$  may be the result of airway–tissue interdependence<sup>136</sup> or a contractile response of the parenchymal tissue itself.<sup>137,138</sup> However, the exact mechanism for increases in  $R_{ti}$  remains a matter of controversy. For example, previous studies have demonstrated that airway heterogeneity can result in an artifactually high  $R_{ti}$ , whether measured directly with alveolar capsules or based on inverse modeling of  $Z_L$ .<sup>8,9,84,110</sup> Nonetheless, information on  $R_{ti}$  may be clinically important to separate those asthmatics whose disease involves primarily airway smooth-muscle constriction from those with a more inflammatory component that may alter or damage the lung tissues.

To answer these questions, Kaczka et al. used the OVW to measure low-frequency  $Z_L$  in 21 asthmatic human subjects during spontaneous bron-

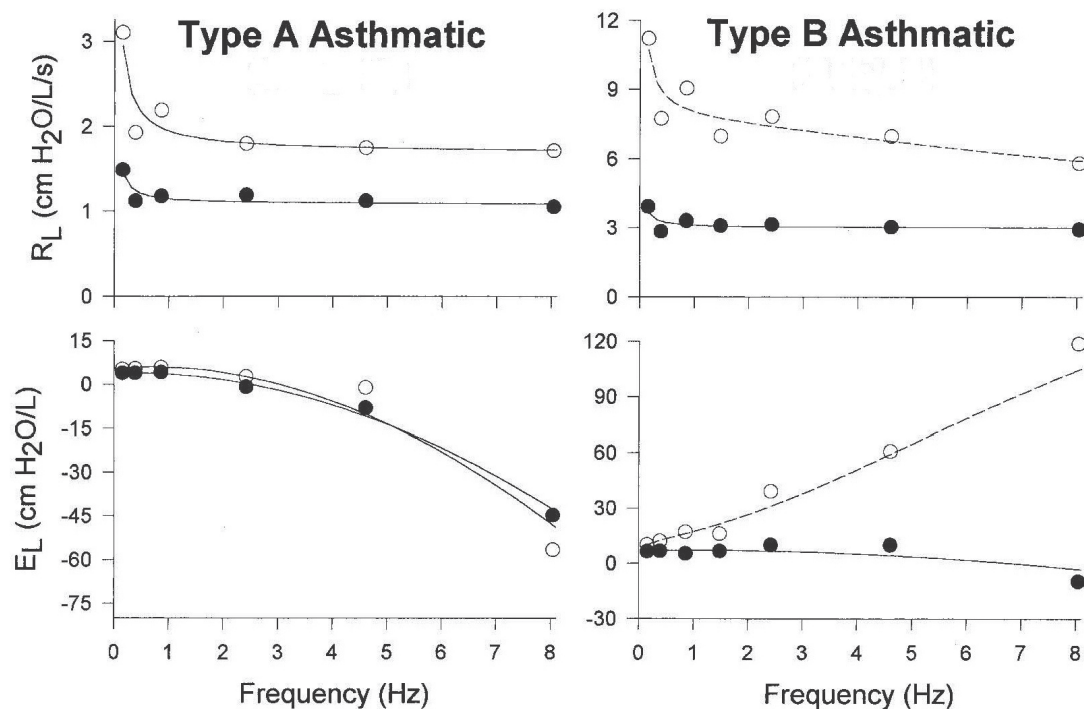


**FIGURE 6:** Examples of lung resistance ( $R_L$ ) and elastance ( $E_L$ ) versus frequency for two representative patients with asthma before (open circles) and following (filled circles) albuterol inhalation. Also shown are corresponding fits using the homogenous airways model of Eq. 9 (solid line) as well as the airway shunt model of Figure 5C (dashed line). Modified from Kaczka et al.,<sup>39</sup> with permission.

choconstriction and following albuterol inhalation.<sup>39</sup> To determine the relative contributions of  $R_{aw}$  and  $R_{ti}$  to  $R_L$  in these subjects, the resulting  $Z_L$  spectra were analyzed in terms of the various model forms shown in Figure 5. These authors demonstrated that asthmatics can be classified into two distinct groups based on their  $Z_L$  spectra (Figure 6). Eleven subjects were classified as Type A asthmatics, displaying slightly elevated  $R_L$  for all frequencies at baseline, but normal  $E_L$ . After albuterol inhalation, their  $R_L$  decreased while  $E_L$  remained unchanged. Their  $Z_L$  data were best described by the homogeneous airways constant-phase model pre- and post-albuterol shown in Figure 5A. The other 10 subjects were classified as Type B asthmatics. They demonstrated highly elevated  $R_L$  at baseline and pronounced positive-frequency dependence in  $E_L$  for frequencies above 2 Hz. The baseline  $Z_L$  data for these subjects were best described by the airway shunt model shown in Figure

5C, consistent with pronounced peripheral airway constriction and shunting of oscillatory flow into the central airway walls. However, post albuterol the  $Z_L$  data of the Type B asthmatics were best described by the homogeneous airways model. Spirometric data were consistent with higher levels of bronchoconstriction in Type B subjects. The inverse model parameters from both groups demonstrated significant reductions in  $R_{aw}$  and  $G$  following albuterol, although only the Type B asthmatics demonstrated significant reductions in  $H$ . More importantly, the percent contributions of  $R_{aw}$  and  $R_{ti}$  to  $R_L$  were similar for both groups, with  $R_{aw}$  contributing about 70% of  $R_L$  near-physiologic breathing frequencies and did not change following albuterol inhalation. Thus, the contribution of  $R_{ti}$  to  $R_L$  appears to be independent of the degree of smooth-muscle constriction. Moreover, this assessment of impedance in human subjects demonstrates the importance of peripheral

airway constriction in the pathophysiology of mild-to-moderate asthma. This has also been confirmed more recently by combining various functional lung imaging techniques (i.e., PET, hyperpolarized MRI) with impedance measurements in asthmatics during bronchoprovocation.<sup>121–123</sup>

## VI. CHRONIC OBSTRUCTIVE PULMONARY DISEASE

Chronic obstructive pulmonary disease (COPD) is associated with irreversible airway obstruction (bronchitis) as well as parenchymal tissue destruction (emphysema). Pulmonary function deteriorates in a slow and progressive manner. Chronic obstructive pulmonary disease (COPD) refers to either chronic bronchitis, emphysema, or a combination of the two.<sup>139</sup> Chronic bronchitis is defined as the presence of a chronic productive cough without a discernible cause for more than half the time over a period of two years. Emphysema is an anatomic diagnosis characterized by a pathological enlargement of air spaces distal to terminal bronchioles and progressive destruction of the alveolar walls. A common factor in the development of emphysema is the reduction in activity of elastase inhibitors, resulting in destruction and disorganization of elastin fibers in the lung. Thus, emphysematous lungs have an increased compliance and a reduced elastic recoil pressure. The destruction of lung parenchyma may cause a loss of radial traction on the airways. This loss of airway tethering, combined with the loss of elastic recoil pressure, enhances the dynamic compression of the airways during expiration, resulting in expiratory flow-limitation (EFL) that can severely compromise tidal breathing. EFL is a central feature of the pathophysiology of COPD. Moreover, it is a highly nonlinear phenomenon in which airflow is no longer dependent on the pressure drop across the airways. Its presence during tidal breathing or forced oscillations obscures the physiologic meaning of linear, time-invariant descriptions of lung mechanics, such as impedance. For example, the effect of bronchodilators in COPD as assessed with impedance is greatly underestimated if EFL is present.<sup>19</sup>

Most techniques used to quantify functional impairment in patients with COPD rely on spirometry, although this can be very nonspecific in distinguishing fixed, bronchitic airway obstruction from premature expiratory airway collapse arising from decreased parenchymal tethering. Nonetheless, the effects of EFL on  $Z_{rs}$  can also be used to provide a sensitive and specific method to detect its presence. In 1993, Peslin et al. reported that during mechanical ventilation, some COPD patients develop large negative swings in respiratory system reactance ( $X_{rs}$ ) measured using FOT.<sup>104</sup> Similar results can also be obtained using a simplified mechanical model of the respiratory system that includes a flow-limiting resistance,<sup>140</sup> as well as in mechanically ventilated rabbits after intravenous methacholine infusion.<sup>103</sup> The reasons for this behavior in reactance has been interpreted as follows: When EFL is present, the linear velocity of gas passing through regions of dynamic airway compression (i.e., choke points) equals the local speed of pressure wave propagation (Figure 7).<sup>141</sup> Under normal conditions, reactance reflects the elastic and inertial properties of the entire respiratory system. However, when EFL is present, the oscillatory signal cannot pass through these choke points and reach the alveoli. Thus flow becomes independent of the driving pressure, and the choke points prevent the propagation of oscillations to the lung periphery. During EFL, impedance reflects the mechanical properties of airways proximal to the choke points, which are much stiffer than those of the periphery. This results in a marked reduction of respiratory compliance, as well as reactance, when measured using FOT (Figure 7).

As a result, FOT can reliably detect EFL by intrabreath variations in  $X_{rs}$  at 5 Hz with 100% specificity and sensitivity compared to the gold standard method that uses analysis of flow and transpulmonary pressure signals.<sup>47,142</sup> Moreover, the measurement of impedance has the advantage of being suitable for the continuous and automatic monitoring of EFL.<sup>143</sup> FOT has also been shown to be reliable during continuous positive airway pressure delivered by nasal mask,<sup>25</sup> opening new perspectives for the automatic adjustment of positive



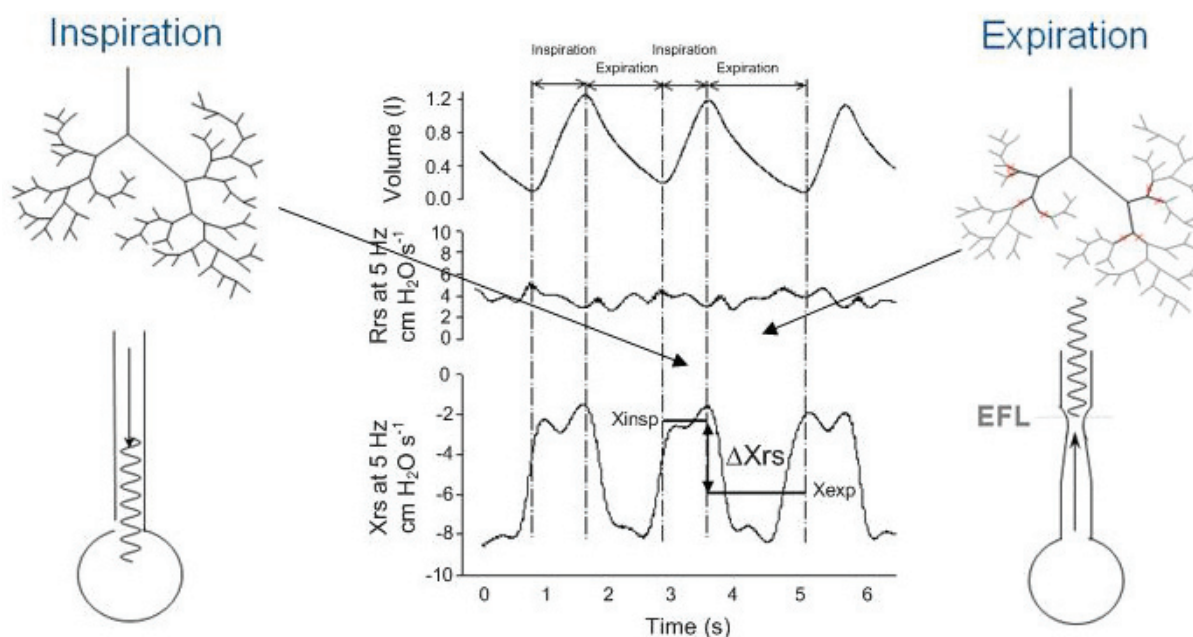


**FIGURE 7:** Volume, resistance ( $R_{rs}$ ), and reactance ( $X_{rs}$ ) tracings in a representative human subject exhibiting expiratory flow-limitation.  $\Delta X_{rs}$  denotes the difference in reactance values measured at the beginning and end of an expiration. EFL: expiratory flow-limitation. Modified from Dellacà et al.,<sup>47</sup> with permission.

end-expiratory pressure (PEEP) during noninvasive mechanical ventilation.

In contrast, Kaczka et al. restricted their analyses of oscillatory pressure-flow relationships in COPD patients to inspiratory periods only, during which EFL nonlinearities were absent. For this study, they introduced the concept of “inspiratory impedance” ( $Z_L^{insp}$ ), a linear and theoretically valid description of lung mechanics that avoids the confounding influence of EFL.<sup>18</sup> To measure  $Z_L^{insp}$ , they proposed the use of a modified OVW, referred to as the enhanced ventilator waveform (EVW). The EVW excites the respiratory system with an inspiratory flow pattern consisting of multiple sinusoids while permitting a patient-driven exhalation to the atmosphere or against externally applied PEEP (Figure 8). The EVW’s ability to measure  $Z_L^{insp}$  while simultaneously maintaining adequate ventilation makes it an ideal tool for assessing inspiratory mechanics in ventilated or flow-limited patients.<sup>23</sup> Kaczka et al. also developed a weighted least-squares technique for computing  $Z_L^{insp}$  from EVW pressure and flow inspirations

and validated it using simulated data as well as data from anesthetized/paralyzed patients.<sup>18</sup>

Figure 9 shows a summary of  $Z_L^{insp}$  data, expressed as inspiratory lung resistance ( $R_L^{insp}$ ) and elastance ( $E_L^{insp}$ ), for two groups of surgical patients under general anesthesia: a control group of six patients with relatively normal lung function undergoing various thorascopic procedures, as well as group of eight patients with severe COPD undergoing lung volume reduction surgery. Measurements were made at PEEPs of 0 and 6 cm H<sub>2</sub>O, immediately after induction of anesthesia but prior to any surgical manipulation. For the control group, PEEP significantly reduced  $R_L^{insp}$  only at the very lowest frequencies. However, for the COPD patients,  $R_L^{insp}$  was reduced at nearly all frequencies with application of PEEP. In addition, PEEP significantly reduced the  $E_L^{insp}$  at the highest frequencies for the COPD group but not in the control group. These data demonstrate that PEEP is beneficial in ventilated COPD patients, specifically by reducing peripheral airway resistance as indicated by the corresponding decrease in  $E_L^{insp}$  at higher frequencies. This is similar to the reduc-

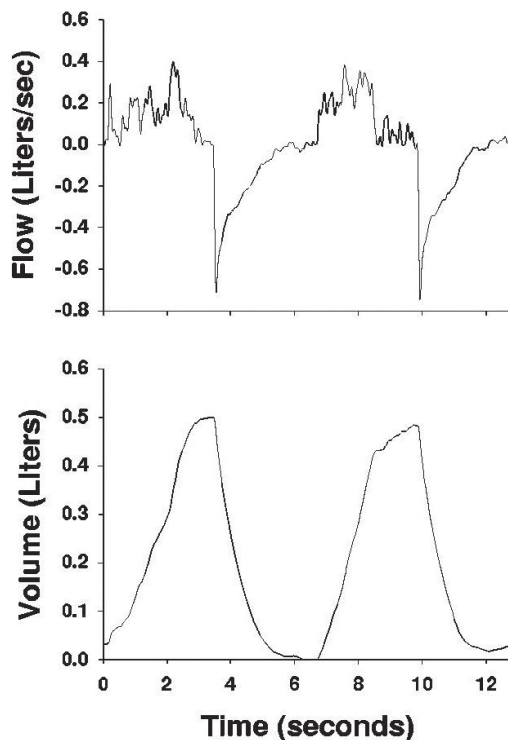


**FIGURE 8:** Flow and volume tracings for enhanced ventilator waveform (EVW), consisting of an inspiratory pattern of multiple sinusoids delivered with a tidal volume of fresh gas, as well a patient-driven exhalation to the atmosphere or against PEEP. Modified from Kaczka et al.,<sup>18</sup> with permission.

tion in peripheral airway constriction in asthmatics following albuterol inhalation (Figure 6).

## VII. ACUTE LUNG INJURY AND ACUTE RESPIRATORY DISTRESS SYNDROME

Acute lung injury (ALI) and the acute respiratory distress syndrome (ARDS) are complex pathologic processes associated with extremely heterogeneous interactions of mechanical and biochemical processes. Both are characterized by widespread airway closure and atelectasis (derecruitment), alveolar flooding, increased lung resistance, and reduced lung compliance.<sup>144</sup> Endotracheal intubation and positive pressure ventilation is the current mainstay of treatment. Nonetheless, the mortality of ALI and/or ARDS is reported to be 30–40%, resulting from overwhelm-

ing sepsis and multiorgan failure.<sup>145</sup> Moreover, artificial ventilation, especially in the presence of heterogeneous regional lung mechanics, can actually worsen the existing injury through two distinct mechanisms. The first is through the overdistribution of lung units from high tidal volumes which are maldistributed (otherwise known as volutrauma), as well as the shear stresses associated with cyclic and repetitive opening and closing of individual lung units (or atelectrauma). Both mechanisms can result in the release of inflammatory cytokines (biotrauma) that may worsen the injury. Consequently, recent emphasis has been on the development of more optimal ventilator protocols, specifically by adjusting PEEP to maximize the recruited lung,<sup>15,146</sup> and tidal volumes or inspiratory pressures to minimize overdistribution.<sup>147</sup> Thus the ability to quantify heterogeneous mechanical derangements during ventilation may provide insight into the ongoing processes of derecruitment, alveolar flooding, and parenchymal overdistribution. Such information may therefore be of use for optimizing parameters such as PEEP, tidal volume, or frequency.

Recent studies in mammalian models of ALI have demonstrated that the frequency-dependent features of impedance can be very sensitive indicators of mechanical heterogeneity in the lungs.<sup>12,23,40,148</sup> Moreover, these studies emphasize the importance of monitoring dynamic elastic properties of the lungs or total respiratory system to assess recruitment and overdistribution during ventilation. For example, Kaczka et al. measured  $Z_{rs}$  in dogs from 0.078 to 8.1 Hz using broadband oscillations over mean airway pressures from 5 to 20 cm H<sub>2</sub>O both at baseline and following oleic acid injury.<sup>40</sup> To assess dynamic elastance and apparent tissue heterogeneity, their  $Z_{rs}$  spectra were fitted with the distributed tissue model of Eq. 13. They found that both the effective dynamic elastance as well as the heterogeneity of tissue mechanics increased following ALI, consistent with derecruitment. However, both of these variables approached preinjury levels as mean airway pressure increased, consistent with the recruitment of lung units.

By contrast, Dellacá et al. demonstrated how within-breath measurements of  $X_{rs}$  at 5 Hz could

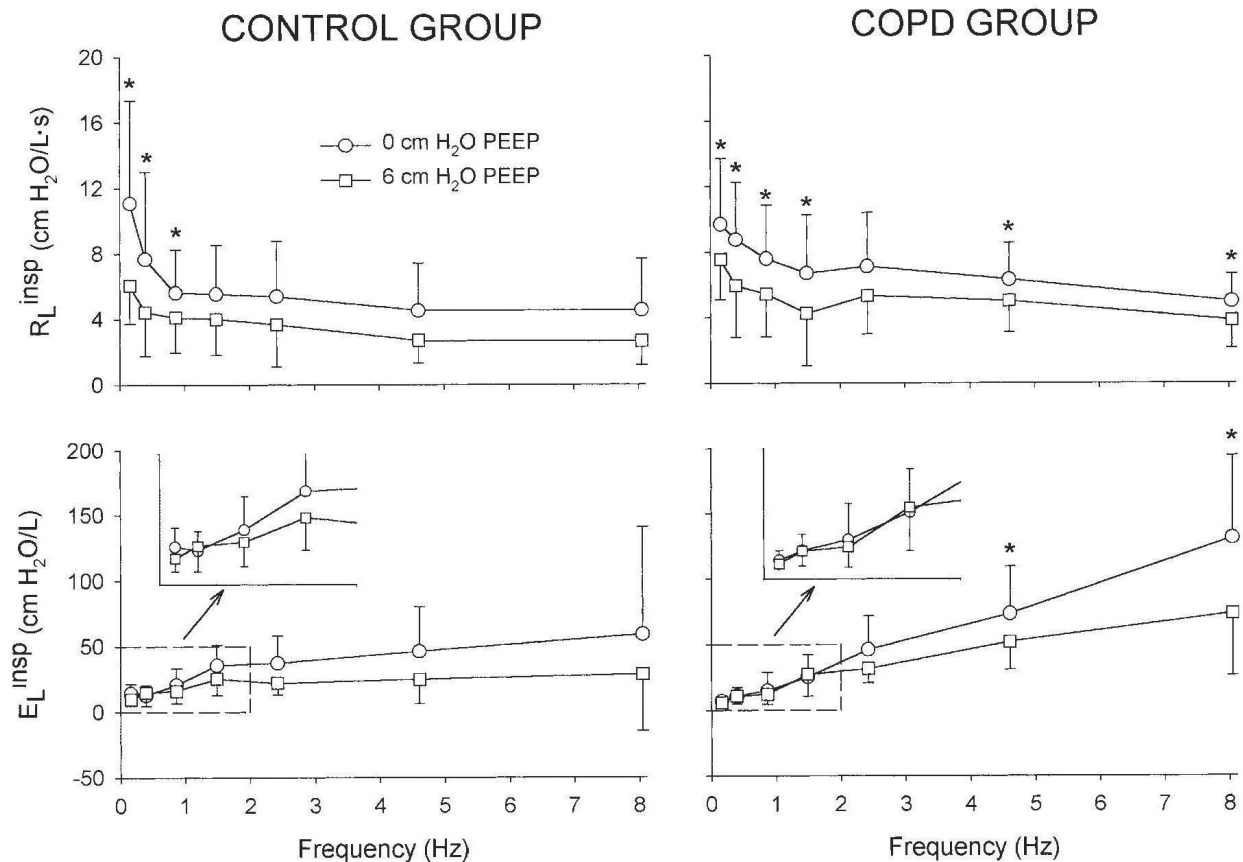


**FIGURE 9:** Comparison of preoperative inspiratory lung resistance and elastance spectra measured with the enhanced ventilator waveform (EVW) (Figure 8) at positive end-expiratory pressures of 0 and 6 cm H<sub>2</sub>O for control subjects (left) and COPD patients (right). \*Significant difference between PEEP levels ( $P < 0.05$ ) via paired t-test. Modified from Kaczka et al.<sup>22</sup> with permission.

be used to monitor recruitment/derecruitment during ventilation in two different porcine models of lung collapse: unilateral absorption atelectasis and bronchoalveolar lavage.<sup>149</sup> They found that changes in the oscillatory compliance at 5 Hz [the reciprocal of dynamic elastance, defined as  $-1/(2\pi \times 5 \times X_{rs})$ ], closely followed the amount of non-aerated tissue volume as measured by Hounsfield density in whole lung computed tomography (CT) scans (Figure 10). They also found a very strong linear relationship between percent derecruitment as determined by CT and oscillatory compliance (Figure 11). Given that single-frequency FOT measurements at 5 Hz allow for a very simple and robust assessments of recruitment in commercially available mechanical ventilators, this technology is potentially useful for

tailoring the ventilatory settings in patients with ALI and/or ARDS.

## VIII. CONCLUSIONS

The unique, frequency-dependent features of the mechanical impedance spectrum for the mammalian respiratory system are exquisitely sensitive to detecting and monitoring the progression of lung disease. In this article, we have reviewed various experimental and theoretical techniques to acquire impedance data in clinical and research settings. We have discussed how such techniques may provide unique insight into pathophysiology and structure-function relationships in asthma, COPD, and ALI.

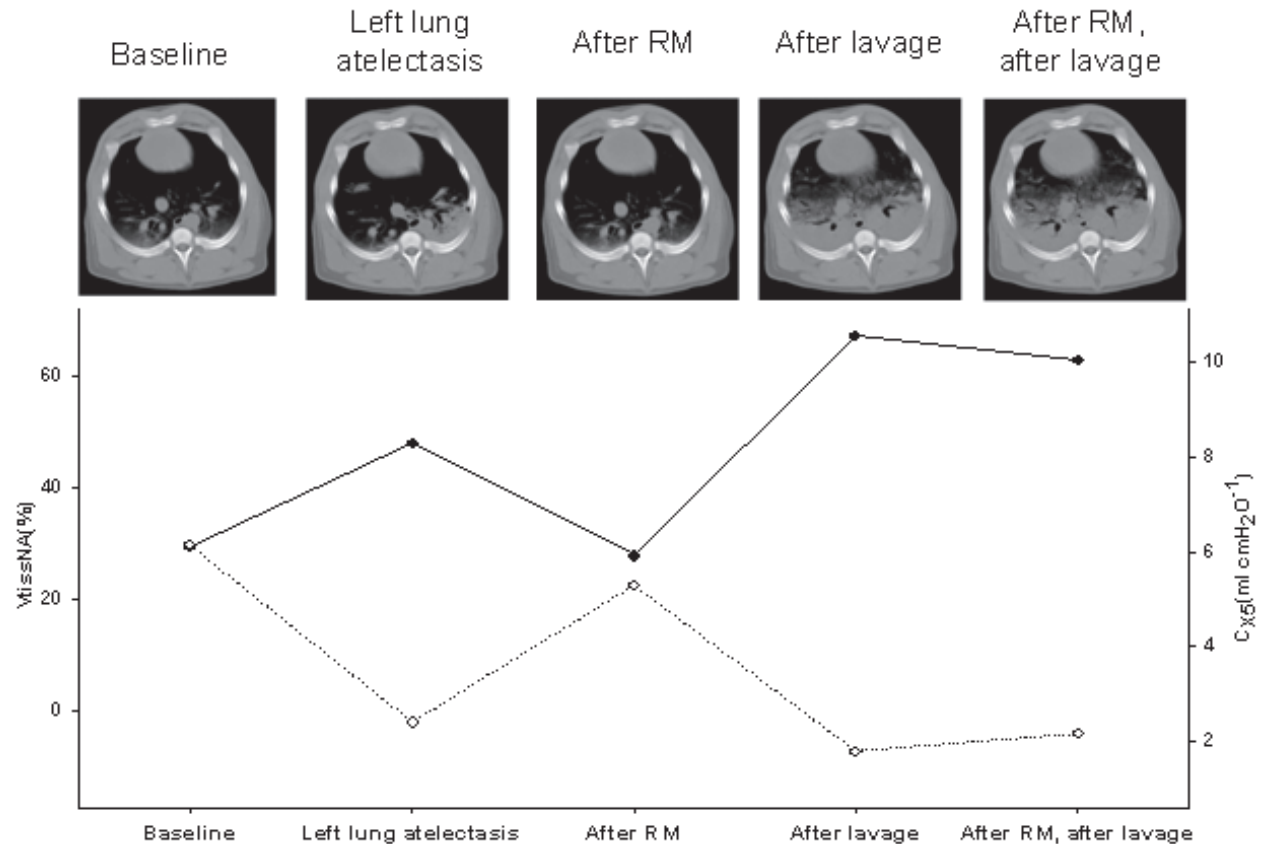


**FIGURE 10:** Upper panel: Computed tomographic scans of a representative animal at baseline, during left-lung atelectasis induced by 10 min of single-lung ventilation at 100% oxygen, after a recruitment maneuver (RM), after bronchoalveolar lavage, and following RM after bronchoalveolar lavage. Lower panel: corresponding non-aerated tissue volume ( $V_{tiss}$ , NA%, closed symbols, solid line) and oscillatory compliance measured at 5 Hz ( $C_{x5}$ , open symbols, dotted line). Modified from Dellaca et al.,<sup>149</sup> with permission.

The interpretation of impedance with inverse models provides even more useful information on functional derangements in the airways and parenchyma, such as bronchoconstriction, expiratory flow-limitation, derecruitment, and overdistention, as well as the efficacy of various treatment protocols. FOT is an ideal diagnostic tool, both to complement more standard tests of pulmonary function, as well as the assessment of lung mechanics in intubated and artificially ventilated patients. Moreover, there exist several physiologic and clinical questions in respiratory medicine for which a robust, noninvasive assessment of mechanical function is required, and we anticipate that FOT will be the ideal technique to address them in the future.

For example, in asthma and COPD, short-term and diurnal variations in airway tone may be sensitive markers of airway instability and impending exacerbations due to the inherent complexities of airway structure and connective tissue matrices.<sup>150</sup> Thus reliable measurements of impedance during quiescent breathing, especially using a portable, home FOT device with telemedicine capabilities,<sup>24,58,59</sup> may be useful for monitoring the dynamics of airway obstruction and its evolution over periods of weeks or months. Such data could provide far more insight into the management and control of obstructive lung diseases when compared to traditional, intermittent clinical assessment.<sup>151</sup>

For patients suffering from ALI and/or ARDS, current ventilator management strategies aim to



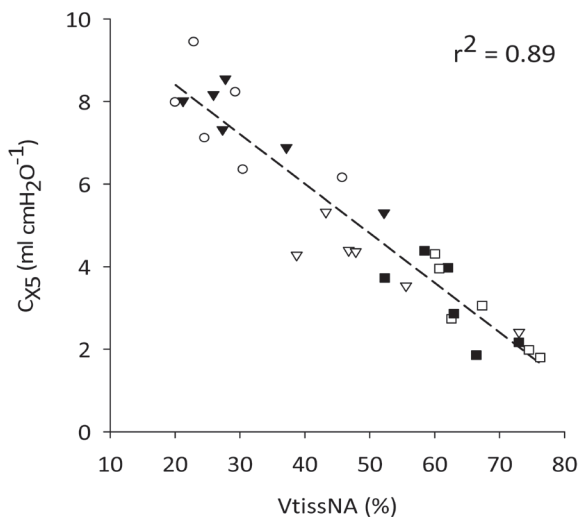


**FIGURE 11:** Correlation between oscillatory compliance measured at 5 Hz ( $C_{x5}$ ) and non-aerated tissue volume ( $V_{tissNA}\%$ ) for six pigs baseline (open circles), during left-lung atelectasis (closed triangles), after recruitment maneuver (RM) (open triangle), after bronchoalveolar lavage (closed squares), and following RM after bronchoalveolar lavage (open squares). Modified from Dellaca et al.,<sup>149</sup> with permission.

maintain inspiratory and expiratory airway pressures within appropriate ranges for sufficient oxygenation and ventilation, while simultaneously minimizing further ventilator associated injury due to parenchymal overdistention and repetitive end-expiratory recruitment and/or derecruitment. While weight-based reduction in tidal volume has been shown to reduce the mortality of ALI and is now largely considered the standard of care,<sup>147</sup> the optimal PEEP to apply to an injured lung is still a matter of considerable controversy.<sup>146,152,153</sup> Because ventilator associated injury is due primarily to the maldistribution of ventilation arising from variations in regional parenchymal mechanics, the ability to quantify lung tissue heterogeneity,<sup>13,40</sup> derecruitment,<sup>149</sup> and overdistention using FOT may have potential for further optimizing ventilatory parameters such as PEEP, tidal volume, or frequency for individual patients. However, clinical trials will be necessary to determine whether such ‘impedance-optimized’ approaches to ventilator management in ALI will result in improved outcomes.

Nonetheless for FOT to find its way into routine use in any clinical arena, future studies combining functional imaging, multi-scale modeling, and oscillatory mechanics will be necessary to determine how specific structural alterations in the lung will affect respiratory impedance assessed with forced oscillations. Such information will be indispensable for the rational development of novel medical and surgical therapies for the treatment of lung disease.

## ACKNOWLEDGMENTS

This work was supported in part by NIH Grant HL089227. The authors thank Dr. Jason H.T. Bates for his helpful criticism during the preparation of the manuscript.

## REFERENCES

1. Mount LE. Variations in the components of the ventilation hindrance of cat lungs. *J Physiol.* 1956;131:393–401.
2. Otis AB, McKerrow CB, Bartlett RA, Mead J, McIlroy MB, Selver-Stone NJ, Radford EP Jr. Mechanical factors in the distribution of pulmonary ventilation. *J Appl Physiol.* 1956;8(4):427–43.
3. Mead J. Contribution of compliance of airways to frequency-dependent behavior of lungs. *J. Appl Physiol.* 1969;26(5):670–73.
4. Macklem PT. Airway obstruction and collateral ventilation. *Physiol Rev.* 1971;51(2):368–436.
5. Hantos Z, Petak F, Adamicza A, Asztalos T, Tolnai J, Fredberg JJ. Mechanical impedances of the lung periphery. *J Appl Physiol.* 1997;83(5):1595–601.
6. Lutchen KR, Greenstein JL, Suki B. How inhomogeneities and airway walls affect frequency dependence and separation of airway and tissue properties. *J Appl Physiol.* 1996;80(5):1696–707.
7. Lutchen KR, Gillis H. Relationship between heterogeneous changes in airway morphometry and lung resistance and elastance. *J Appl Physiol.* 1997;83(4):1192–201.
8. Lutchen KR, Suki B, Zhang Q, Petak F, Daroczy B, Hantos Z. Airway and tissue mechanics during physiological breathing and bronchoconstriction in dogs. *J Appl Physiol.* 1994;77(1):373–85.

9. Lutchen KR, Hantos Z, Petak F, Adamicza A, Suki B. Airway inhomogeneities contribute to apparent lung tissue mechanics during constriction. *J Appl Physiol*. 1996;80(5):1841–49.
10. Petak F, Hantos Z, Adamicza A, Daroczy B. Partitioning of pulmonary impedance: modeling vs. alveolar capsule approach. *J Appl Physiol*. 1993;75(2):513–21.
11. Hyatt RE, Scanlon PD, Nakamura M. Interpretation of pulmonary function tests: a practical guide. 3d ed. Philadelphia, PA: Lippincott, Williams & Wilkins; 2009.
12. Kaczka DW, Brown RH, Mitzner W. Assessment of heterogeneous airway constriction in dogs: a structure–function analysis. *J Appl Physiol*. 2009;106(2):520–30.
13. Kaczka DW, Cao K, Christensen GE, Bates JHT, Simon BA. Analysis of regional mechanics in canine lung injury using forced oscillations and 3-D image registration. *Ann Biomed Eng*. 2011;39(3):1112–24.
14. Tgavalekos NT, Venegas JG, Suki B, Lutchen KR. Relation between structure, function, and imaging in a three-dimensional model of the lung. *Ann Biomed Eng*. 2003;31(4):363–73.
15. Bellardine Black CL, Hoffman AM, Tsai LW, Ingenito EP, Suki B, Kaczka DW, Simon BA, Lutchen KR. Impact of positive end-expiratory pressure during heterogeneous lung injury: insights from computed tomographic image functional modeling. *Ann Biomed Eng*. 2008;36(6):980–91.
16. Goldman MD. Clinical application of forced oscillation. *Pulm Pharmacol Ther*. 2001;14(5):341–50.
17. Tawfik B, Chang HK. A nonlinear model of respiratory mechanics in emphysematous lungs. *Ann Biomed Eng*. 1988;16:159–74.
18. Kaczka DW, Ingenito EP, Lutchen KR. Technique to determine inspiratory impedance during mechanical ventilation: implications for flow-limited patients. *Ann Biomed Eng*. 1999;27:340–55.
19. Dellacà RL, Pompilio PP, Walker PP, Duffy N, Pedotti A, Calverley PM. Effect of bronchodilation on expiratory flow limitation and resting lung mechanics in COPD. *Eur Respir J*. 2009;33(6):1329–37.
20. Bates JHT, Irvin CG. Time dependence of recruitment and derecruitment in the lung: a theoretical model. *J Appl Physiol*. 2002;93:705–13.
21. Maksym GN, Bates JHT. A distributed nonlinear model of lung tissue elasticity. *J Appl Physiol*. 1997;82(1):32–41.
22. Kaczka DW, Ingenito EP, Body SC, Duffy SE, Mentzer SJ, DeCamp MM, Lutchen K. Inspiratory lung impedance in COPD: effects of PEEP and immediate impact of lung volume reduction surgery. *J Appl Physiol*. 2001;90:1833–41.
23. Bellardine CL, Ingenito EP, Hoffman A, Lopez F, Sanborn W, Suki B, Lutchen KR. Heterogeneous airway versus tissue mechanics and their relation to gas exchange function during mechanical ventilation. *Ann Biomed Eng*. 2005;33(5):626–41.
24. Dellacà RL, Gobbi A, Pastena M, Pedotti A, Celli B. Home monitoring of within-breath respiratory mechanics by a simple and automatic forced oscillation technique device. *Physiol Meas*. 2010;31(4):N11–N24.
25. Dellacà RL, Rotger M, Aliverti A, Navajas D, Pedotti A, Farré R. Noninvasive detection of expiratory flow limitation in COPD patients during nasal CPAP. *Eur Respir J*. 2006;27(5):983–91.
26. Peslin R, Fredberg JJ. Oscillation mechanics of the respiratory system. In: Macklem PT, Mead J, editors. *Handbook of physiology: the respiratory system*. Bethesda, MD: American Physiological Society; 1986. p. 145–78.
27. LaPrad AS, Lutchen KR. Respiratory impedance measurements for assessment of lung mechanics: focus on asthma. *Respir Physiol Neurobiol*. 2008;163(1–3):64–73.
28. Oostveen E, MacLeod D, Lorino H, Farré R, Hantos Z, Desager K, Marchal F; ERS Task Force on Respiratory Impedance Measurements. The forced oscillation technique in clinical practice: methodology, recommendations and future developments. *Eur Respir J*. 2003;22(6):1026–41.
29. Lutchen KR, Suki B. Understanding Pulmonary Mechanics Using the Forced Oscillations Technique. In: Khoo, editor. *Approaches to Pulmonary Physiology and Medicine*. New York: Plenum Press; 1996. p. 227–53.
30. MacLeod D, Birch M. Respiratory input impedance measurement: forced oscillation methods. *Med Biol Eng Comput*. 2001;39(5):505–16.
31. DuBois AB, Brody AW, Lewis DH, Burgess BF Jr. Oscillation mechanics of lungs and chest in man. *J Appl Physiol*. 1956;8:587–94.
32. Bates JHT. Pulmonary mechanics: a system identification perspective. Annual International Conference of the IEEE Engineering in Medicine and Biology Society. 2009 Sep 2–6, Minneapolis, MN. 2009:170–72.

33. Bates JHT. Lung mechanics: an inverse modeling approach. New York: Cambridge University Press; 2009.
34. Michaelson ED, Grassman ED, Peters W. Pulmonary mechanics by spectral analysis of forced random noise. *J Clin Invest.* 1975;56: 1210–30.
35. Pedley TJ, Schroter RC, Sudlow MF. The prediction of pressure drop and variation of resistance within the human bronchial airways. *Respir Physiol.* 1970;9:387–405.
36. Fredberg JJ, Stamenovic D. On the imperfect elasticity of lung tissue. *J Appl Physiol.* 1989;67(6): 2408–19.
37. Barnas GM, Yoshino K, Loring SH, Mead J. Impedance and relative displacements of relaxed chest wall up to 4 Hz. *J Appl Physiol.* 1987;62(1):71–81.
38. Kaczka DW, Ingenito EP, Suki B, Lutchen KR. Partitioning airway and lung tissue resistances in humans: effects of bronchoconstriction. *J Appl Physiol.* 1997;82(5):1531–41.
39. Kaczka DW, Ingenito EP, Israel E, Lutchen KR. Airway and lung tissue mechanics in asthma: effects of albuterol. *Am J Resp Crit Care Med.* 1999;159:169–78.
40. Kaczka DW, Hager DN, Hawley ML, Simon BA. Quantifying mechanical heterogeneity in canine acute lung injury: impact of mean airway pressure. *Anesthesiology* 2005;103:306–17.
41. Welch PD. The use of fast Fourier transform for the estimation of power spectra: a method based on time averaging over short, modified periodograms. *IEEE Trans Audio Electroacoustics* 1967;15(2):70–73.
42. Farre R, Rotger M, Navajas D. Optimized estimation of respiratory impedance by signal averaging in the time domain. *J Appl Physiol.* 1992;73(3): 1181–89.
43. Lutchen KR, Guiridenella CA, Jackson AC. Inability to separate airway from tissue properties using input impedance in humans. *J Appl Physiol.* 1990;68(6):2403–12.
44. Bates JHT. Lung mechanics—the inverse problem. *Austral Phys Eng Sci Med.* 1991;14(4):197–203.
45. Similowski T, Bates JHT. Two-compartment modelling of respiratory system mechanics at low frequencies: gas redistribution or tissue rheology? *Eur Respir J.* 1991;4:353–58.
46. Mount LE. The ventilation flow-resistance and compliance of rat lungs. *J Physiol.* 1955;127(1): 157–67.
47. Dellacà RL, Santus P, Aliverti A, Stevenson N, Centanni S, Macklem PT, Pedotti A, Calverley PM. Detection of expiratory flow limitation in COPD using the forced oscillation technique. *Eur Respir J.* 2004;23(2):232–40.
48. Suki B, Barabasi A-L, Lutchen KR. Lung tissue viscoelasticity: a mathematical framework and its molecular basis. *J Appl Physiol.* 1994;76(6): 2749–59.
49. Melo PL, Werneck MM, Giannella-Neto A. Linear servo-controlled pressure generator for forced oscillation measurements. *Med Biol Eng Comput.* 1998;36:11–16.
50. Farre R, Rotger M, Montserrat JM, Navajas D. A system to generate simultaneous forced oscillation and continuous positive airway pressure. *Eur Respir J.* 1997;10:1349–53.
51. Navajas D, Farre R, Canet J, Rotger M, Sanchis J. Respiratory input impedance in anesthetized paralyzed patients. *J Appl Physiol.* 1990;69(4): 1372–79.
52. Navajas D, Farre R. Forced oscillation assessment of respiratory mechanics in ventilated patients. *Crit Care* 2001;5:3–9.
53. Navajas D, Farré R, Rotger M, Badia R, Puig-de-Morales M, Montserrat JM. Assessment of airflow obstruction during CPAP by means of forced oscillation in patients with sleep apnea. *Am J Resp Crit Care Med.* 1998;157(5):1526–30.
54. Simon BA, Mitzner W. Design and calibration of a high-frequency oscillatory ventilator. *IEEE Trans Biomed Eng.* 1991;38(2):214–18.
55. Schuessler TF, Bates JHT. A computer-controlled research ventilator for small animals: design and evaluation. *IEEE Trans Biomed Eng.* 1995;42(9): 860–66.
56. Kaczka DW, Lutchen KR. Servo-controlled pneumatic pressure oscillator for respiratory impedance measurements and high frequency ventilation. *Ann Biomed Eng.* 2004;32(4):596–608.
57. Hantos Z, Daroczy B, Suki B, Galgoczy G, Csentes T. Forced oscillatory impedance of the respiratory system at low frequencies. *J Appl Physiol.* 1986;60(1):123–32.
58. Rigau J, Farré R, Roca J, Marco S, Herms A, Navajas D. A portable forced oscillation device for respiratory home monitoring. *Eur Respir J.* 2002;19(1):146–50.
59. Rigau J, Burgos F, Hernández C, Roca J, Navajas D, Farré R. Unsupervised self-testing of airway

- obstruction by forced oscillation at the patient's home. *Eur Respir J*. 2003;22(4):668–71.
60. Jackson AC. Dynamic response of transducers used in respiratory physiology. In: Otis AB, editor. *Techniques in the life sciences*. Shannon, Clare, Ireland: Elsevier Scientific Publishers Ireland Ltd.; 1984. p. 1–18.
  61. Delavault E, Saumon G, Georges R. Identification of transducer defect in respiratory impedance measurements by forced random noise. Correction of experimental data. *Respir Physiol*. 1980;40:107–17.
  62. Mead J, Gaensler EA. Esophageal and pleural pressures in man, upright and supine. *J Appl Physiol*. 1959;14(1):81–83.
  63. Macklem PT, Mead J. Resistance of central and peripheral airways measured by a retrograde catheter. *J Appl Physiol*. 1967;22(3):395–401.
  64. Fredberg JJ, Keefe DH, Glass GM, Castile RG, Frantz ID 3rd. Alveolar pressure nonhomogeneity during small-amplitude high-frequency oscillation. *J Appl Physiol*. 1984;57(3):788–800.
  65. Kaminsky DA, Irvin CG, Lundblad L, Moriya HT, Lang S, Allen J, Viola T, Lynn M, Bates JH. Oscillation mechanics of the human lung periphery in asthma. *J Appl Physiol*. 2004;97(5):1849–58.
  66. Duvivier C, Rotger M, Felicio da Silva J, Peslin R, Navajas D. Static and dynamic performances of variable reluctance and piezoresistive pressure transducers for forced oscillation measurements. *Eur Resp Rev*. 1991;1(3):146–50.
  67. Farre R, Peslin R, Navajas D, Gallina C, Suki B. Analysis of the dynamic characteristics of pressure transducers for studying respiratory mechanics at high frequencies. *Med Biol Eng Comput*. 1980;27:531–37.
  68. Sullivan WJ, Peters GM, Enright PL. Pneumotachographs: theory and clinical application. *Respiratory Care*. 1984;29(7):736–49.
  69. Suter SP, Skalak R. The history of Poiseuille's Law. *Ann Rev Fluid Mech*. 1993;25:1–19.
  70. Grenvik A, Hedstrand U, Sjorgren H. Problems in pneumotachography. *Acta Anaesthesiologica Scandinavica*. 1966;10(3):147–55.
  71. Habre W, Asztalos T, Sly PD, Petak F. Viscosity and density of common anaesthetic gases: implications for flow measurements. *Br J Anaesth*. 2001;87(4):602–07.
  72. Finucane KE, Egan BA, Dawson SV. Linearity and frequency response of pneumotachographs. *J Appl Physiol*. 1972;32(1):121–26.
  73. Jackson AC, Vinegar A. A technique for measuring frequency response of pressure, volume, and flow transducers. *J Appl Physiol*. 1979;47(2):462–67.
  74. Pelle G, Lorino H, Perez J, Lorino AM, Harf A. Modeling of the transfer function of the flow transducer used in ventilatory measurements. *IEEE Trans Biomed Eng*. 1984;31(4):356–61.
  75. Renzi PE, Giurdanella CA, Jackson AC. Improved frequency response of pneumotachometers by digital compensation. *J Appl Physiol*. 1990;68(1):382–86.
  76. Farre R, Navajas D, Peslin R, Rotger M, Duvivier C. A correction procedure for the asymmetry of differential pressure transducers in respiratory impedance measurements. *IEEE Trans Biomed Eng*. 1989;36(11):1137–40.
  77. Hager DN, Fuld M, Kaczka DW, Fessler HE, Brower RG, Simon BA. Four methods of measuring tidal volume during high-frequency oscillatory ventilation. *Crit Care Med*. 2006;34(3):751–57.
  78. Ligeza P. Constant-bandwidth constant-temperature hot-wire anemometer. *Rev Sci Instr*. 2007;78(7):075104.
  79. Plakk P, Liik P, Kingisepp PH. Hot-wire anemometer for spirometry. *Med Biol Eng Comput*. 1998;36:17–21.
  80. Lundsgaard JS, Grønlund J, Einer-Jensen N. Evaluation of a constant-temperature hot-wire anemometer for respiratory-gas-flow measurements. *Med Biol Eng Comput*. 1979;17:211–15.
  81. Barnas GM, Mills PJ, Mackenzie CF, Ashby M, Sexton WL, Imle PC, Wilson PD. Dependencies of respiratory system resistance and elastance on amplitude and frequency in the normal range of breathing. *Am Rev Respir Dis*. 1991;143:240–44.
  82. Barnas GM, Sprung J, Craft TM, Williams JE, Ryder IG, Yun JA, Mackenzie CF. Effect of lung volume on lung resistance and elastance in awake subjects measured sinusoidal forcing. *Anesthesiology*. 1993;78(6):1082–90.
  83. Barnas GM, Delaney PA, Gheorghiu I, Mandava S, Russell RG, Kahn R, Mackenzie CF. Respiratory impedances and acinar gas transfer in a canine model for emphysema. *J Appl Physiol*. 1997;83(1):179–88.
  84. Bates JHT, Lauzon A-M, Dechman GS, Maksym GN, Schuessler TF. Temporal dynamics of pulmonary response to intravenous histamine in dogs: effects of dose and lung volume. *J Appl Physiol*. 1994;76(2):616–26.



85. Daroczy B, Hantos Z. Generation of optimum pseudorandom signals for respiratory impedance measurements. *Int J Biomed Comput.* 1990;25:21–31.
86. Cooley JW, Tukey JW. An algorithm for the machine calculation of complex Fourier series. *Math Comput.* 1965;19:297–301.
87. Kaczka DW, Barnas GM, Suki B, Lutchen KR. Assessment of time-domain analyses for estimation of low-frequency respiratory mechanical properties and impedance spectra. *Ann Biomed Eng.* 1995;23:135–51.
88. Maki BE. Interpretation of the coherence function when using pseudorandom inputs to identify nonlinear systems. *IEEE Trans Biomed Eng.* 1986;33(8):775–79.
89. Suki B, Hantos Z, Daroczy B, Alkaysi G, Nagy S. Nonlinearity and harmonic distortion of dog lungs measured by low-frequency forced oscillations. *J Appl Physiol.* 1991;71(1):69–75.
90. Daroczy B, Fabula A, Hantos Z. Use of noninteger-multiple pseudorandom excitation to minimize nonlinear effects on impedance estimation. *Eur Resp Rev.* 1991;1(3):183–87.
91. Suki B, Lutchen KR. Pseudorandom signals to estimate apparent transfer and coherence functions of nonlinear systems: applications to respiratory mechanics. *IEEE Trans Biomed Eng.* 1992;39(11):1142–51.
92. Lutchen KR, Yang K, Kaczka DW, Suki B. Optimal ventilation waveforms for estimating low-frequency respiratory impedance. *J Appl Physiol.* 1993;75(1):478–88.
93. Lutchen KR, Kaczka DW, Suki B, Barnas G, Cevenini G, Barbini P. Low-frequency respiratory mechanics using ventilator-driven forced oscillations. *J Appl Physiol.* 1993;75(6):2549–60.
94. Lutchen KR. Direct use of mechanical ventilation to measure respiratory mechanics associated with physiological breathing. *Eur Resp Rev.* 1994;19:f198–202.
95. Chapman FW, Newell JC. Estimating lung mechanics of dogs with unilateral lung injury. *IEEE Trans Biomed Eng.* 1989;36(4):405–13.
96. Peslin R, Ying Y, Gallina C, Duvivier C. Within-breath variations of forced oscillation resistance in healthy subjects. *Eur Respir J.* 1992;5(1):86–92.
97. Horowitz JG, Siegel SD, Primiano FPJ, Chester EH. Computation of respiratory impedance from forced sinusoidal oscillations during breathing. *Comput Biomed Res.* 1983;16(6):499–521.
98. Cauberghs M, Van de Woestijne KP. Changes of respiratory input impedance during breathing in humans. *J Appl Physiol.* 1992;73(6):2355–62.
99. Avanzolini G, Barbini P. A comparative evaluation of three on-line identification methods for a respiratory mechanical model. *IEEE Trans Biomed Eng.* 1985;32(11):957–63.
100. Avanzolini G, Barbini P, Cappello A, Cevenini G. Real-time tracking of parameters of lung mechanics: emphasis on algorithm tuning. *J Biomed Eng.* 1990;12:489–95.
101. Jensen A, Atileh H, Suki B, Ingenito EP, Lutchen KR. Selected contribution: airway caliber in healthy and asthmatic subjects: effects of bronchial challenge and deep inspirations. *J Appl Physiol.* 2001;91:506–15.
102. Lauzon A-M, Bates JHT. Estimation of time-varying respiratory mechanical parameters by recursive least squares. *J Appl Physiol.* 1991;71(3):1159–65.
103. Vassiliou M, Peslin R, Saunier C, Duvivier C. Expiratory flow limitation during mechanical ventilation detected by the forced oscillation method. *Eur Respir J.* 1996;9:779–86.
104. Peslin R, Felicio da Silva J, Duvivier C, Chabot F. Respiratory mechanics studied by forced oscillations during artificial ventilation. *Eur Respir J.* 1993;6:772–84.
105. Baldi S, Dellacà R, Govoni L, Torchio R, Aliverti A, Pompilio P, Corda L, Tantucci C, Gulotta C, Brusasco V, Pellegrino R. Airway distensibility and volume recruitment with lung inflation in COPD. *J Appl Physiol.* 2010;109(4):1019–26.
106. Pellegrino R, Pompilio PP, Bruni GI, Scano G, Crimi C, Biasco L, Coletta G, Cornara G, Torchio R, Brusasco V, Dellacà RL. Airway hyperresponsiveness with chest strapping: A matter of heterogeneity or reduced lung volume? *Respir Physiol Neurobiol.* 2009;66(1):47–53.
107. Hantos Z, Daroczy B, Csendes T, Suki B, Nagy S. Modeling of low-frequency pulmonary impedance in dogs. *J Appl Physiol.* 1990;68(3):849–60.
108. Ingenito EP, Davison B, Fredberg JJ. Tissue resistance in the guinea pig at baseline and during methacholine constriction. *J Appl Physiol.* 1993;75(6):2541–48.
109. Tepper R, Sato J, Suki B, Martin JG, Bates JHT. Low-frequency pulmonary impedance in rabbits and its response to inhaled methacholine. *J Appl Physiol.* 1992;73(1):290–95.

110. Hantos Z, Daroczy B, Suki B, Nagy S, Fredberg JJ. Input impedance and peripheral inhomogeneity of dog lungs. *J Appl Physiol.* 1992;72(1):168–78.
111. Hildebrandt J. Comparison of mathematical models for cat lung and viscoelastic balloon derived by Laplace transform methods from pressure-volume data. *Bull Math Biophys.* 1969;31:651–67.
112. Hantos Z, Daroczy B, Klebniczki J, Dombos K, Nagy S. Parameter estimation of transpulmonary mechanics by a nonlinear inertive model. *J Appl Physiol.* 1982;52(4):955–63.
113. Daroczy B, Hantos Z. An improved forced oscillatory estimation of respiratory impedance. *Int J Bio-Med Comput.* 1982;13:221–35.
114. Kaczka DW, Massa CB, Simon BA. Reliability of estimating stochastic lung tissue heterogeneity from pulmonary impedance spectra: a forward-inverse modeling study. *Ann Biomed Eng.* 2007;35(10):1722–38.
115. Bates JHT, Allen G. The estimation of lung mechanics parameters in the presence of pathology: a theoretical analysis. *Ann Biomed Eng.* 2006;34(3):384–92.
116. Lutchen KR, Jensen A, Atileh H, Kaczka DW, Israel E, Suki B, Ingenito EP. Airway constriction pattern is a central component of asthma severity: the role of deep inspirations. *Am J Resp Crit Care Med.* 2001;164:207–15.
117. Schwartz BL, Anafi RC, Aliyeva M, Thompson-Figueroa JA, Allen GB, Lundblad LK, Bates JH. Effects of central airway shunting on the mechanical impedance of the mouse lung. *Ann Biomed Eng.* 2011;39(1):497–507.
118. Suki B, Yuan H, Zhang Q, Lutchen KR. Partitioning of lung tissue response and inhomogeneous airway constriction at the airway opening. *J Appl Physiol.* 1997;82(4):1349–59.
119. Ito S, Ingenito EP, Arold SP, Parameswaran H, Tgavalekos NT, Lutchen KR, Suki B. Tissue heterogeneity in the mouse lung: effects of elastase treatment. *J Appl Physiol.* 2004;204–12.
120. Lorx A, Szabó B, Hercsuth M, Péntzes I, Hantos Z. Low-frequency assessment of airway and tissue mechanics in ventilated COPD patients. *J Appl Physiol.* 2009;107(6):1884–92.
121. Tgavalekos NT, Tawhai M, Harris RS, Musch G, Vidal-Melo M, Venegas JG, Lutchen KR. Identifying airways responsible for heterogeneous ventilation and mechanical dysfunction in asthma: an image functional modeling approach. *J Appl Physiol.* 2005;99(6):2388–97.
122. Tgavalekos NT, Musch G, Harris RS, Vidal Melo MF, Winkler T, Schroeder T, Callahan R, Lutchen KR, Venegas JG. Relationship between airway narrowing, patchy ventilation and lung mechanics in asthmatics. *Eur Respir J.* 2007;29(6):1174–81.
123. Campana L, Kenyon J, Zhalehdoust-Sani S, Tzeng YS, Sun Y, Albert M, Lutchen KR. Probing airway conditions governing ventilation defects in asthma via hyperpolarized MRI image functional modeling. *J Appl Physiol.* 2009;106(4):1293–300.
124. Lutchen KR. Sensitivity analysis of respiratory parameter uncertainties: impact of criterion function form and constraints. *J Appl Physiol.* 1990;69(2):766–75.
125. Yuan H, Suki B, Lutchen KR. Sensitivity analysis for evaluating nonlinear models of lung mechanics. *Ann Biomed Eng.* 1998;26:230–41.
126. Fredberg JJ, Inouye D, Miller B, Nathan M, Jafari S, Raboudi SH, Butler JP, Shore SA. Airway smooth muscle, tidal stretches, and dynamically determined contractile states. *Am J Resp Crit Care Med.* 1997;156:1752–59.
127. Dwyer JM, editor. Beta agonists in the management of asthma. 1st ed. Providence, RI: New England and Regional Allergy Proceedings; 1986.
128. Jenne JW, Tashkin DP. Beta-adrenergic agonists. In: Weiss EB, Stein M, editors. *Bronchial asthma.* Boston: Little Brown; 1993. p. 700–48.
129. Bachofen H. Lung tissue resistance in normal and asthmatic subjects. *Helv Med Acta.* 1966;2:108–21.
130. Bachofen H, Scherrer M. Lung tissue resistance in healthy subjects and in patients with lung disease. In: Bouhuys A, editor. *Airway dynamics.* Springfield, IL: Thomas; 1970. p. 123–34.
131. Marshall R, DuBois AB. The viscous resistance of lung tissue in patients with pulmonary disease. *Clin Sci.* 1956;15:473–83.
132. Ludwig MS, Romero PV, Bates JHT. A comparison of the dose-response behavior of canine airways and parenchyma. *J Appl Physiol.* 1989;67(3):1220–25.
133. Ludwig MS, Robatto FM, Sly PD, Browman M, Bates JHT, Romero PV. Histamine-induced constriction of canine peripheral lung: an airway or tissue response? *J Appl Physiol.* 1991;71(1):287–93.
134. Romero PV, Ludwig MS. Maximal methacholine-induced constriction in rabbit lung: interactions between airways and tissue? *J Appl Physiol.* 1991;70(3):1044–50.

135. Romero PV, Robatto FM, Simard S, Ludwig MS. Lung tissue behavior during methacholine challenge in rabbits in vivo. *J Appl Physiol.* 1992;73(1): 207–12.
136. Mitzner W, Blosser S, Yager D, Wagner E. Effect of bronchial smooth muscle contraction on lung compliance. *J Appl Physiol.* 1992;72(1):158–67.
137. Fredberg JJ, Bunk D, Ingenito E, Shore SA. Tissue resistance and contractile state of lung parenchyma. *J Appl Physiol.* 1993;74(3):1387–97.
138. Kapanci Y, Assimacopoulos A, Irle C, Zwahlen A, Gabbiani G. Contractile interstitial cells in pulmonary alveolar septa: a possible regulator of ventilation/perfusion ratio? *J Cell Biol.* 1974;60: 375–92.
139. West JB. *Pulmonary pathophysiology: the essentials.* 7th ed. Baltimore, MD: Lippincott, Williams & Wilkins, 2008.
140. Peslin R, Farre R, Rotger M, Navajas D. Effect of expiratory flow limitation on respiratory mechanical impedance: a model study. *J Appl Physiol.* 1996;81(6):2399–406.
141. Dawson SV, Elliott EA. Wave-speed limitation on expiratory flow—a unifying concept. *J Appl Physiol.* 1977;43(3):498–515.
142. Mead J, Whittenberger JL. Physical properties of human lungs measured during spontaneous breathing. *J Appl Physiol.* 1953;5:779–96.
143. Dellacà RL, Duffy N, Pompilio PP, Aliverti A, Koulouris NG, Pedotti A, Calverley PM. Expiratory flow limitation detected by forced oscillation and negative expiratory pressure. *Eur Respir J.* 2007;29(2):363–74.
144. Bernard GR, Artigas A, Brigham KL, Carlet J, Falke K, Hudson L, Lamy M, LeGall JR, Morris A, Spragg R. Report of the American–European Consensus conference on acute respiratory distress syndrome: definitions, mechanisms, relevant outcomes, and clinical trial coordination. *J Crit Care.* 1994;9(1):72–81.
145. Ware LB, Matthay MA. The acute respiratory distress syndrome. *N Engl J Med.* 2000;342:1334–49.
146. Brower RG, Lanken PN, MacIntyre N, Matthay MA, Morris A, Ancukiewicz M, Schoenfeld D, Thompson BT; National Heart, Lung, and Blood Institute ARDS Clinical Trials Network. Higher versus lower positive end-expiratory pressures in patients with the acute respiratory distress syndrome. *N Engl J Med.* 2004;351(4):327–36.
147. The Acute Respiratory Distress Syndrome Network. Ventilation with lower tidal volumes as compared with traditional tidal volumes for acute lung injury and the acute respiratory distress syndrome. *N Engl J Med.* 2000;342(18):1301–08.
148. Bellardine Black CL, Hoffman AM, Tsai LW, Ingenito EP, Suki B, Kaczka DW, Simon BA, Lutchen KR. Relationship between dynamic respiratory mechanics and disease heterogeneity in sheep lavage injury. *Crit Care Med.* 2007;35(3):870–78.
149. Dellaca RL, Andersson Olerud M, Zannin E, Kostic P, Pompilio PP, Hedenstierna G, Pedotti A, Frykholm P. Lung recruitment assessed by total respiratory system input reactance. *Intensive Care Med.* 2009;35:2164–72.
150. Frey U, Suki B. Complexity of chronic asthma and chronic obstructive pulmonary disease: implications for risk assessment, and disease progression and control. *Lancet.* 2008;372(9643):1088–99.
151. Frey U, Brodbeck T, Majumdar A, Taylor DR, Town GI, Silverman M, Suki B. Risk of severe asthma episodes predicted from fluctuation analysis of airway function. *Nature* 2005;438(7068):667–70.
152. Talmor D, Sarge T, Malhotra A, O'Donnell CR, Ritz R, Lisbon A, Novack V, Loring SH. Mechanical ventilation guided by esophageal pressure in acute lung injury. *N Engl J Med.* 2008;359(20):2095–104.
153. Talmor DS, Fessler HE. Are esophageal pressure measurements important in clinical decision-making in mechanically ventilated patients? *Respiratory Care.* 2010;55(2):162–72.

